

Analyzing the effects of complete tropical forest removal on the regional climate using a detailed three-dimensional energy budget: An application to Africa

Peter K. Snyder and Jonathan A. Foley

Center for Sustainability and the Global Environment, Nelson Institute for Environmental Studies,
University of Wisconsin-Madison, Madison, Wisconsin, USA

Department of Atmospheric and Oceanic Sciences, University of Wisconsin-Madison, Madison, Wisconsin, USA

Matthew H. Hitchman

Department of Atmospheric and Oceanic Sciences, University of Wisconsin-Madison, Madison, Wisconsin, USA

Christine Delire¹

Center for Sustainability and the Global Environment, Nelson Institute for Environmental Studies,
University of Wisconsin-Madison, Madison, Wisconsin, USA

Received 17 December 2003; revised 22 June 2004; accepted 13 July 2004; published 4 November 2004.

[1] Previous studies have indicated how tropical deforestation can have a significant influence on regional and global climate through altered biophysical exchanges of water, energy, and momentum at the land-atmosphere boundary. However, the mechanisms for translating a surface forcing to changes in the atmospheric thermodynamics and circulation have not received as much attention. Here we present a new moist static energy budget method for examining the regional atmospheric response to removal of tropical forests and how land surface forcing is propagated into the atmosphere. A detailed three-dimensional grid cell energy budget approach is used within a coupled atmosphere-biosphere model (Community Climate Model, Version 3–Integrated Biosphere Simulator (CCM3-IBIS)) to identify how land surface forcing affects the regional climate through the vertical and horizontal movement of moist static energy. This approach allows us to clearly identify where the moist static energy budget changes, which mechanisms are responsible for the changes, and how energy moves to adjacent areas and affects rainfall. Generally, replacement of the tropical forests with bare soil in the model leads to decreased rainfall in the tropics due to regional drying, while enhanced rainfall occurs in the subtropics associated with strengthened monsoon winds importing more moisture. Interesting regional complexities emerge, notably in tropical Africa. There, removal of the forests leads to lower rainfall near the coast but enhanced rainfall in central tropical Africa. This approach provides a useful diagnostic tool for examining the implications of land use and land cover change on the regional and global atmospheric thermodynamics and circulation. *INDEX TERMS*: 3322 Meteorology and Atmospheric Dynamics: Land/atmosphere interactions; 3309 Meteorology and Atmospheric Dynamics: Climatology (1620); 3307 Meteorology and Atmospheric Dynamics: Boundary layer processes; *KEYWORDS*: land-atmosphere interactions, tropical deforestation, Africa, shallow/deep convection, climate modeling, biophysical processes

Citation: Snyder, P. K., J. A. Foley, M. H. Hitchman, and C. Delire (2004), Analyzing the effects of complete tropical forest removal on the regional climate using a detailed three-dimensional energy budget: An application to Africa, *J. Geophys. Res.*, *109*, D21102, doi:10.1029/2003JD004462.

1. Introduction

[2] The impact of land use and land cover change on regional and global climate is of considerable concern as global population and development pressures continue to mount. A large portion of the Earth's surface has already been modified for croplands, pastureland, forest harvesting, and urban and industrial development. Almost 35% of the

¹Now at Institut des Sciences de l'Evolution, Université Montpellier II, Montpellier, France.

land surface (nearly 55 million km²) has been directly converted to human-dominated systems [Ramankutty and Foley, 1999], while other large areas are heavily influenced by human activities. Of the remaining land surface, the large and ecologically sensitive tropical rain forests of South America, Africa, and Southeast Asia may be most at risk owing to population and development pressures and the increasing demand for natural resources from these regions.

[3] Land use and land cover change affect the complex biophysical interactions that occur between vegetation and the atmosphere and are extremely important in driving the climate system across the regional and global scales. Vegetation and soils exchange water, energy, and momentum with the atmosphere. As a result, changes in the land surface properties can modify these surface fluxes and have a large effect on Earth's climate through changes in the atmospheric thermodynamics and circulation. Furthermore, changes in the climate from land surface forcing in any particular region may affect distant regions as well through the effects of atmospheric transport and teleconnections.

[4] The influence of land use and land cover change on the climate may be especially strong in the tropical forests of South America, Africa, and Southeast Asia, where the vegetation plays an important role in the cycling of water and the atmospheric transport of energy to the extratropics. There have been many modeling-based case studies exploring the influence of tropical forest land use and land cover change on climate. Early research by Dickinson and Henderson-Sellers [1988], for example, examined the role of tropical deforestation in the Amazon on the regional climate using a land surface model coupled to an atmospheric general circulation model (AGCM). The biophysical changes in the aerodynamic roughness and the corresponding reduction in the turbulent exchange of water, energy, and momentum between the surface and the planetary boundary layer were quantified, as well as changes to the surface radiation budget and the water cycle. They found that deforestation of the Amazon resulted in a temperature increase of 3°–5°C when forested land was converted to grassland. More recent tropical deforestation studies have produced a variety of results; however, all the studies found a warming of the surface air temperature and a reduction in evapotranspiration, and almost all found a reduction in precipitation [Charney, 1975; Dickinson and Henderson-Sellers, 1988; Lean and Warrilow, 1989; Nobre et al., 1991; Dickinson and Kennedy, 1992; Eltahir and Bras, 1993; Henderson-Sellers et al., 1993; Lean and Rowntree, 1993; Xue and Shukla, 1993; Polcher and Laval, 1994; Eltahir, 1996; Zeng et al., 1996; Costa and Foley, 2000; Snyder et al., 2004].

[5] In certain ecosystems, land use and land cover change have the potential for greatly affecting the environment through biophysical feedbacks. Wang and Eltahir [2000a, 2000b, 2000c] found that land use change in the Sahel may alter the climate enough such that the remaining vegetation could be subject to climatic conditions outside its optimal growing environment. Furthermore, work by Pielke et al. [2002] and Marland et al. [2003] suggests that in some cases the biophysical effects of land use change may be as important as the biogeochemical effects on the global climate.

[6] The tropical forests of South America, Africa, and Southeast Asia are coincident with the convective heating

centers that define the large regions of deep moist convection in the atmosphere. These regions transfer large amounts of latent energy from the surface through canopy transpiration, evaporation of canopy-intercepted water, and soil evaporation. This moisture is transported to higher levels in the atmospheric column where the energy is released through condensation. The energy that is transported aloft is eventually redistributed to other tropical regions as well as to the extratropics through the Hadley circulation and by the steady and anomalous forcing of Rossby waves [James, 1994].

[7] Removal of the tropical rain forests can have a considerable impact not only on the regional energy balance but also on the regional-scale climate. This can result in moisture and energy convergence in areas outside of the surface forcing. Changes in the land surface properties and surface energy fluxes can also modify the distribution and intensity of deep convection that cause changes in the high-level outflow and may influence the extratropics through atmospheric teleconnections [Sud et al., 1988; Polcher, 1995; Sud et al., 1996; Zhang et al., 1996; Chase et al., 2000; Pielke, 2001; Zhao et al., 2001; Werth and Avissar, 2002]. Such potential extratropical influences include modulation of the Arctic Oscillation, the North Atlantic Oscillation, and the Pacific–North American pattern. However, discussion of the extratropical response to removal of the tropical forest biome is outside the scope of this paper.

[8] Although these studies have improved our understanding of the influence of tropical forests on the climate system, there is still a gap in our knowledge about how changes in the land surface relate to changes in the regional and global circulation. Specifically, simple cause-and-effect relationships have been established whereby a given surface forcing results in a change in the regional and global climate, even though the exact mechanisms connecting the different scales may not be well understood. To begin to understand how vegetation acts to modify the regional and global climate, it is necessary to have a careful three-dimensional accounting of the energy storage and transfer in the atmosphere both horizontally and vertically and to track changes in the surface energy budget up through the planetary boundary layer and the atmospheric column. By tracking the changes in energy from the surface to the regional and global scales, one can identify the coupling mechanisms that act to propagate a signal to locations removed from the surface forcing.

[9] The goal of this sensitivity study is to present a new method for understanding how the three-dimensional atmospheric energy budget changes as a result of tropical forest removal and how this relates to changes in climatic forcing mechanisms at regional scales. We have devised a three-dimensional energy accounting method that determines the change in the total atmospheric energy budget and the individual energy budget components for the atmosphere. Analysis of the individual energy budget components is used to identify physical processes that are important for a region and to help explain how they can alter the climate of regions far removed from the surface forcing.

[10] We conduct our energy budget analysis within a fully coupled atmosphere-biosphere modeling system consisting of an AGCM and a detailed land surface/ecosystem model. Simulations were performed wherein the tropical forests of

Table 1. Equivalent Pressure and Height for Each Sigma Level in the Model^a

Model Level	Pressure Level, hPa	Height, km
1	5	36.0
2	15	29.4
3	30	23.4
4	65	19.2
5	100	16.7
6	135	14.8
7	180	13.0
8	240	11.2
9	305	9.5
10	385	7.9
11	470	6.3
12	560	5.0
13	650	3.8
14	735	2.7
15	810	1.9
16	865	1.3
17	905	0.9
18	925	0.8

^aPressure and height represent the midpoint of the level and are an average of the three African regions during the September–October–November (SON) season.

South America, Africa, and Southeast Asia are intact and wherein the tropical forests were completely removed and replaced with desert (bare soil). The response of the three-dimensional energy budget and climate to removal of the tropical forests is evaluated by comparison of the two simulations. Although our simulation explores the response of the climate system to pantropical forest removal, we focus much of our analysis on changes to the energy budget over tropical Africa as a detailed illustration of this approach.

[11] We acknowledge that complete tropical forest removal is unrealistic and unlikely to occur in the tropics; however, this approach does help to establish the upper bounds of the effects using a complex global model and presents a method from which more realistic sensitivity studies can be directly applied. While complete removal of the tropical forest vegetation may represent the upper bounds of the vegetation's effect on the climate system as represented by an AGCM, higher-resolution mesoscale models may be able to better represent the finer-scale circulation changes caused by a heterogeneous landscape. For example, using a mesoscale atmosphere model, *Baidya Roy and Avissar* [2002] have shown that sporadic deforestation of the tropical rain forest can actually lead to an increase in precipitation as local circulation changes caused by differential heating of the heterogeneous land surface combined with already humid air can enhance the development and organization of moist convection. Therefore partial deforestation may, in fact, represent the maximum influence of the vegetation's influence on the climate system. Clearly, further research is needed to understand how land surface heterogeneity and its representation at different spatial scales affects moist convective processes.

[12] Section 2 describes the modeling framework used in this study, section 3 presents the energy balance approach developed, and section 4 describes the specifics of the simulation design. The general results of the tropical forest removal simulation are outlined in section 5, while the

detailed analysis of three-dimensional energy budget changes in Africa is presented in section 6. A summary of the three-dimensional energy budget analysis is presented in section 7, followed by a more general summary and conclusions in section 8.

2. Description of the Coupled Atmosphere-Biosphere Model, CCM3-IBIS

[13] We use the coupled atmosphere-biosphere model, Community Climate Model, Version 3.2–Integrated Biosphere Simulator (CCM3-IBIS) [*Delire et al.*, 2002]. The atmospheric component of the coupled model is the Community Climate Model, Version 3.2 [*Kiehl et al.*, 1998]. CCM3 is a fully dynamic atmospheric model that supports a variety of spatial resolutions, 18 vertical levels, and a 20-min time step. CCM3 includes a precipitation model that includes both shallow and deep convective schemes as well as large-scale precipitation estimates. This revised precipitation model eliminates the overactive hydrology of the CCM2 model and more accurately portrays precipitation and convective processes [*Hack et al.*, 1998]. The vertical coordinate system of CCM3 uses a terrain-following hybrid sigma-pressure system, and all results presented in this paper use the model level for the vertical coordinate with the equivalent pressure provided where applicable. The approximate equivalent tropical Africa average pressure and altitude of the model levels are given in Table 1.

[14] CCM3 is coupled to the Integrated Biosphere Simulator version 2.1 [*Foley et al.*, 1996; *Kucharik et al.*, 2000]. IBIS is a global model of land surface and terrestrial ecosystem processes that represents the physical, physiological, and ecological processes occurring in vegetation and soils in a coherent and semimechanistic way. IBIS simulates land surface processes (energy and water balance), vegetation phenology (budburst and senescence), and vegetation dynamics (competition between vegetation types). IBIS calculates these processes on a spatial and temporal scale consistent with that of the AGCM spatial and temporal resolutions. IBIS represents vegetation as two layers (taller “trees” and short “shrubs” and “grasses”). In IBIS a grid cell can contain one or more plant functional types (PFTs) that together comprise a vegetation type [*Foley et al.*, 1996]. For example, the tropical evergreen forest vegetation type (that is part of the tropical forest biome) is dominated by the tropical evergreen tree PFT but also contains the tropical broadleaf deciduous tree PFT as well as some shrub and grass PFTs. Soil is represented with six layers in the model and simulates temperature, water, and ice content down to a depth of 4 m. Canopy photosynthesis is realistically modeled using the C₃ and C₄ physiology scheme of *Farquhar et al.* [1980]. Canopy stomatal conductance [*Collatz et al.*, 1991, 1992] and respiration [*Amthor*, 1984] are also calculated to establish a link between the vegetation and the atmospheric budgets for the exchange of energy and water. Budburst and senescence are determined by climatic factors.

[15] We run the model with a fixed vegetation distribution, so that vegetation structure and biogeography are not allowed to change in response to the climate. IBIS uses a

prescribed “potential vegetation” distribution representing the vegetation that would exist in the absence of anthropogenic land use change [Ramankutty and Foley, 1999]. To date, tropical deforestation has claimed $\sim 28\%$ of the tropical forests and just over 16% of the savanna vegetation [Ramankutty and Foley, 1999; Food and Agricultural Organization, 2001]. The soil texture, important for soil moisture, is defined in IBIS according to the *International Geosphere-Biosphere Programme Data and Information System* [1999] global gridded texture database. The variability of the soil texture across the model domain affects the movement of water through the soil and the availability of water to the vegetation.

3. Description of the Three-Dimensional Energy Budget Calculations

[16] We use a combination of the nonadvective form of the moist static energy and a grid cell energy budget approach to track changes in the three-dimensional energy budget of the atmosphere as a result of tropical forest removal. Changes in the moist static energy are a useful proxy of a cause-and-effect relationship because they represent the changes in temperature, moisture, and mass throughout the atmospheric column as a result of land surface forcing. However, it is often difficult to identify how changes at a specific location and level are due to changes in the surface forcing versus contributions from outside the region of forcing. Therefore we develop a three-dimensional energy budget approach in order to identify how changes in the energy of the atmospheric column affect the climate. This technique can be used to distinguish between changes in energy within the atmospheric column and changes due to advective feedbacks. Finally, we use this approach to illustrate the limitations of the nonadvective form of the moist static energy as a diagnostic tool in biosphere-atmosphere processes.

[17] The moist static energy of an air parcel is defined as the sum of its enthalpy, gravitational potential energy, and latent heat content. In our analysis we calculate the moist static energy (E) for all grid cells as

$$E = C_p T + \Phi + L_v q, \quad (1)$$

where C_p is the specific heat of air at constant pressure, T is the air temperature of the grid cell, Φ is the geopotential energy, L_v is the latent heat of vaporization, and q is the specific humidity of the grid cell. By comparing the moist static energy of the deforested and control simulations we can identify the regions that are affected by the surface forcing.

[18] We calculate the total energy budget and store each of the individual components for each grid volume in the model. Our definition of the grid volume energy budget is as follows. Starting with the total energy equation (2) for a volume of air as defined by Gill [1982],

$$\frac{\partial \left[\rho \left(C_p T + \frac{1}{2} \mathbf{U}^2 + \Phi + L_v q \right) \right]}{\partial t} = -\nabla \cdot \mathbf{F}^{\text{tot}} + Q_H, \quad (2)$$

where

$$\mathbf{F}^{\text{tot}} = \rho \mathbf{U} \left(C_p T + \frac{1}{2} \mathbf{U}^2 + \Phi + L_v q \right) + P \mathbf{U} + \mathbf{F}^{\text{rad}} - k \nabla T - \mu \nabla \left(\frac{1}{2} \mathbf{U}^2 \right) \quad (3)$$

$$Q_H = \rho L_v \frac{Dq}{Dt}; \quad (4)$$

ρ is the density of the air; T is the air temperature; \mathbf{U} is the velocity of the zonal, meridional, and vertical wind; Φ is the geopotential energy; q is the specific humidity; C_p is the specific heat at constant pressure; and L_v is the latent heat of vaporization. The total energy equation (2) states that the time rate of change of internal, kinetic, gravitational potential, and latent energy of the grid volume is equal to the convergence of the total energy flux ($-\nabla \cdot \mathbf{F}^{\text{tot}}$) (equation (3)) plus the latent heating rate (Q_H) (equation (4)). The total energy flux (equation (3)) contains (from left to right) the advective flux of internal, kinetic, gravitational potential and latent energy; the rate of work by pressure forces; the radiative flux; the diffusion of heat flux; and the diffusion of kinetic energy flux. To a first approximation, several of these terms in equation (3) can be neglected since they are of a much smaller magnitude than the main energy terms [Gill, 1982]. Those that can be ignored include the advective flux of kinetic energy, the rate of work by pressure forces, and the diffusion of heat and kinetic energy flux terms. After simplifying equation (3) one is left with

$$\text{EB} = \rho L_v \frac{Dq}{Dt} - \nabla \cdot \mathbf{F}^{\text{rad}} - \nabla \cdot \rho \mathbf{U} (C_p T + \Phi + L_v q), \quad (5)$$

where the total three-dimensional energy budget (EB) terms are (from left to right) the latent heat content due to phase changes, the convergence of radiative heat, and the convergence of the internal, gravitational potential, and latent energy fluxes.

[19] The units in equation (5) are in W m^{-3} and can be thought of as an energy density per unit time or a power density. By integrating throughout the atmospheric column, equation (5) represents the total energy contained within the atmospheric column in more traditional units (W m^{-2}) familiar to the atmospheric sciences. By integrating through just the lowest level of the model the sensitivity of the energy budget quantity in equation (5) to changes in the surface fluxes of net radiation and latent and sensible heating can be identified. If the level of free convection and the level of neutral buoyancy were known in the model, integration between these two levels would yield a quantity analogous to the convective available potential energy (CAPE): a useful metric representing the amount of buoyant energy available to accelerate a parcel vertically that is important for identifying changes in moist tropical convection. Since we are not specifically evaluating parcel velocities or the altitude of penetration, CAPE cannot easily be determined. However, the relationship between changes to the EB and CAPE could be additionally useful for identifying how convective activity is influenced by changes to the surface and boundary layer energy budgets.

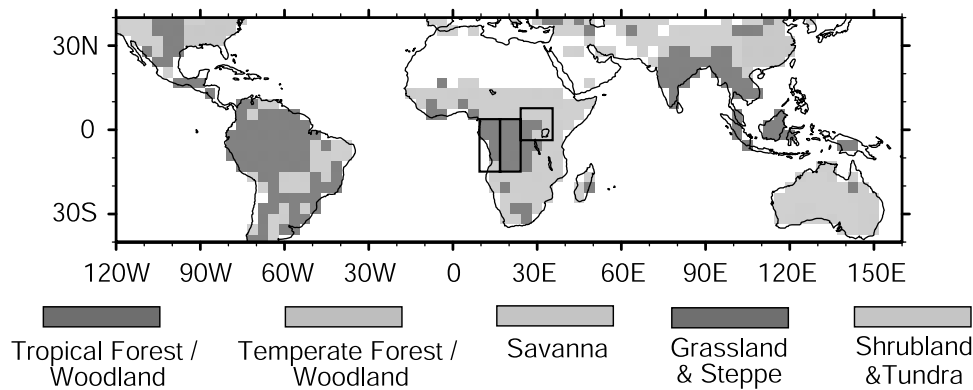


Figure 1. Tropical distribution of the five potential vegetation biomes defined in this study at T31 spatial resolution. Each biome includes one or more vegetation types as defined in the IBIS land surface model. Boxed areas in Africa represent averaging areas and are identified from west to east as regions 1, 2, and 3. See color version of this figure at back of this issue.

[20] In the CCM3-IBIS model we calculate each of the terms in the total energy budget equation for each model time step and average them over a month. Therefore we store 13 energy budget terms for a given grid volume: the convergence of the zonal, meridional, and vertical fluxes of internal, geopotential, and latent energy; the convergence of the shortwave and longwave radiative fluxes; the energy associated with heating due to phase changes; and the total energy budget comprising the 12 terms. These diagnostic variables are calculated in the model using state variables and a simple finite difference approximation method. Because of our use of the finite-differencing approximation, no vertical energy terms are calculated for the top and bottom layers of the atmospheric model. Therefore total energy budget results are not presented for the top or bottom layers (levels 1 and 18); however, they can be inferred from changes in the other energy budget variables and the vertical velocity at the surface. While the convergence of the shortwave and longwave radiative fluxes as well as the energy associated with phase change (equation (4)) terms are included in the total EB, the individual components are not plotted as they are an order of magnitude smaller than the horizontal and vertical advection terms.

4. Simulation Design

[21] In order to determine the role that the tropical forest ecosystem has on climate, we compare a simulation of tropical forest removal against a control simulation with intact tropical forest cover. For the tropical forest removal simulation we replaced the tropical evergreen forest and woodland cells, tropical deciduous forest and woodland cells, and all cells of the mixed forest and woodland class that fall within the northern and southern extent of the tropical forest biome with desert (Figure 1). The area of forest removal as represented in the model is just under 23,000,000 km², or ~16% of the Earth's land surface area. The control run uses a potential vegetation distribution (all biomes intact and in their "natural" locations) as indicated by *Ramankutty and Foley* [1999]. Replacement of the tropical forests in the simulation means that a given cell's vegetation is removed and replaced with desert (bare soil). On average, the conversion of tropical forest cover to bare

ground increases the land surface albedo from roughly 0.13 to 0.17 annually.

[22] Both simulations were run at a spectral resolution of T31 (~3.75° × 3.75° latitude/longitude grid). All atmospheric and most land surface calculations were run at a temporal resolution of 20 min. In order to isolate the response of the vegetation alone we ran the simulations with climatologically prescribed sea surface temperatures (SSTs) and a fixed atmospheric CO₂ concentration of 350 ppmv. While we acknowledge that prescribed SSTs are not as physically representative as interactive SSTs, it is necessary to limit what can change so that we may isolate the climate forcing due to removal of a particular vegetation type. However, there are certainly important feedbacks operating between the biosphere, atmosphere, and ocean that must be represented for a more detailed and realistic modeling of the climate system as a whole.

[23] Both simulations were run for 20 years. The last 10 years of each run are used for averaging. Results presented in this paper are significant at the 95% confidence level using a Student's *t* test unless specified otherwise. The statistical significance was computed independently for the monthly, seasonal, and annual results. Vertical profiles for the African regions represent horizontal averages and use all cells contained within the region regardless of statistical significance.

5. Overview of Climate Response to Pantropical Forest Removal

[24] Removal of the tropical forests leads to a reduction in total evapotranspiration due to the replacement of trees with grasses or, in our case, desert. Total evapotranspiration is made up of upper and lower canopy transpiration, evaporation of canopy-intercepted water, and soil evaporation. Although soil evaporation increases once the covering vegetation is gone, its rate is less than the combined rates of canopy transpiration and evaporation of canopy-intercepted water (Table 2). The combination of transpiration and evaporation of canopy-intercepted water in the vegetated case is greater than the rate of soil evaporation in the vegetation removal case because the plant draws water from

Table 2. Selected Results From the Tropical Forest Removal Simulation^a

Variable	All Tropical		All Tropical (Control)		Africa	
	SON	Annual	SON	Annual	SON	Annual
Temperature, K	1.6	1.2	297.6	297.0	1.1	1.1
Net radiation, W m ⁻²	-25.3	-19.9	135.4	127.7	-34.2	-26.2
Albedo, fraction	0.05	0.04	0.13	0.13	0.06	0.05
Latent heat flux, W m ⁻²	-41.9	-30.4	109.2	101.2	-46.1	-34.6
Sensible heat flux, W m ⁻²	15.1	11.0	28.0	27.9	8.5	8.3
Specific humidity, g kg ⁻¹	-2.3	-1.5	14.3	13.6	-2.6	-1.6
Precipitation, mm d ⁻¹	-2.1	-1.5	6.4	5.5	-3.2	-1.8
Total evapotranspiration, mm d ⁻¹	-1.5	-1.1	3.8	3.5	-1.6	-1.2
Canopy transpiration, mm d ⁻¹	[-1.6]	[-1.6]	1.6	1.6	[-1.1]	[-1.6]
Evaporation of canopy-intercepted water, mm d ⁻¹	[-2.0]	[-1.7]	2.0	1.7	[-2.1]	[-1.8]
Soil evaporation, mm d ⁻¹	2.3	2.3	0.1	0.1	1.9	2.2
PBL height, m	153.1	52.7	656.6	677.3	186.6	42.4
Total cloud cover, fraction	-0.12	-0.07	0.75	0.70	-0.17	-0.08
Low-level cloud cover, fraction	-0.07	-0.06	0.25	0.26	-0.06	-0.04
Medium-level cloud cover, fraction	0.02	0.02	0.1	0.09	0.04	0.03
High-level cloud cover, fraction	-0.11	-0.06	0.66	0.59	-0.20	-0.09

^aResults are presented as differences (tropical forest removal minus control) and are averaged for the SON season and averaged annually for the entire tropical forest biome and the Africa region. Control simulation results are provided for the entire biome for comparison. Difference results averaged using only values significant at the 95% significance level using a two-sided Student's *t* test. All variables shown represent surface-level values except the planetary boundary layer height ("PBL height") and the four "cloud cover" variables. Canopy transpiration and evaporation of canopy-intercepted water difference terms shown in brackets represent the raw difference, not the statistically significant values, since these terms are constant at zero for the length of the tropical forest removal model run.

deeper reservoirs in the soil and evaporates water intercepted by the canopy. With soil evaporation, there is less water to draw from as evaporation only occurs in the thin top layer of soil. The surface albedo increases with tropical forest removal, and there is a reduction in net radiation that acts to cool the surface; however, the effect of reduced evapotranspiration is much larger than the albedo effect and the surface temperature increases. Lower net evapotranspiration rates lead to a drier planetary boundary layer as less water is transported to the atmosphere from the surface. Moisture convergence can act to partially offset the reduction; however, the overall result is that the atmosphere dries, less precipitation falls, and water recycling is reduced.

[25] We evaluate the overall climate response to removal of the tropical forests by analyzing several climatological fields averaged over the entire tropical forest for the September–October–November (SON) season and over the entire year (Table 2). Each of the variables behaves as expected; there is a warming of the land surface, a greatly reduced latent heat flux (or evapotranspiration rate), an increase in the surface albedo, reduced net radiation, reduced cloud cover, and less precipitation and water cycling back to the atmosphere as the low-level specific humidity is reduced. The reduction in evapotranspiration results from decreases in canopy transpiration and evaporation of canopy-intercepted water despite an increase in soil evaporation. These results are in general agreement with a study by *Xue and Shukla* [1993] and with those results as summarized by *Costa and Foley* [2000]. It should be noted, however, that most of the tropical deforestation studies as referenced in this paper replace the tropical forest vegetation with some type of residual vegetation (e.g., grasslands or shrublands), while in our simulations we have no residual vegetation (i.e., bare soil).

[26] Figure 2a shows the simulated surface temperature response to tropical forest removal across the tropics. Here the surface temperature warms considerably over all three

tropical forest centers as latent cooling is severely reduced with removal of the vegetation. In contrast, there is a slight cooling over the west coast of Africa and over various equatorial regions of the ocean.

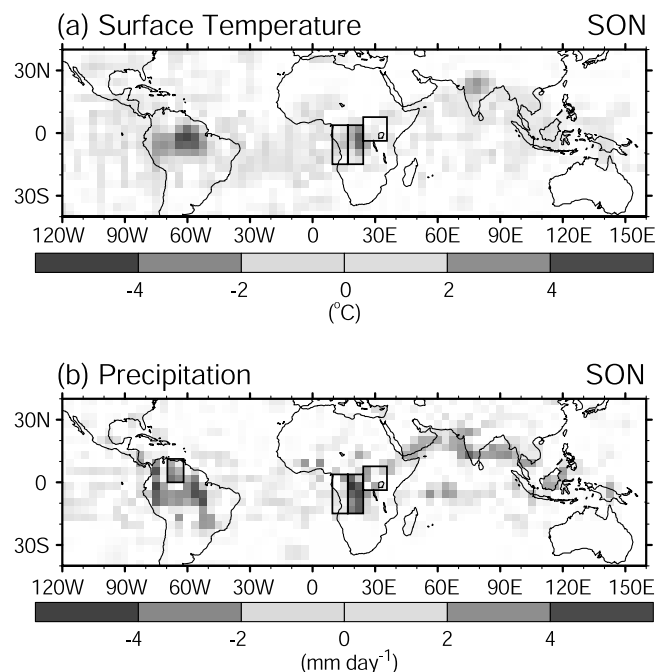


Figure 2. Tropical distribution of September–October–November (SON) changes in (a) surface temperature (°C) and (b) precipitation (mm day⁻¹) due to tropical forest removal. Differences (tropical forest removal minus control) are shown only for cells significant at the 95% significance level using a two-sided Student's *t* test. Boxed regions in Africa are defined in Figure 1. The boxed region in South America on the precipitation map represents the area referenced in Figure 9. See color version of this figure at back of this issue.

[27] Figure 2b shows the change in precipitation with tropical forest removal. In most cases the precipitation is greatly reduced (25% annually and 33% in SON) as there is less energy and moisture available for driving deep tropical convection. Worth noting are the areas of increased precipitation in the northern part of the Amazon basin, northeast of the tropical forest region in Africa, and numerous regions along the northern perimeter of the Indian Ocean. The cells located over the ocean (e.g., the Bay of Bengal) where there is an increase in precipitation are artifacts from using fixed SSTs in the model. In this case, the enhanced low-level winds caused by the reduced land surface roughness with vegetation removal increase evaporation of the ocean surface and lead to a greater flux of moisture into the atmosphere. With interactive SSTs, mixing of the thermocline would occur, thus bringing cooler water to the surface and inhibiting as large a flux of moisture into the atmosphere.

[28] The subtropical regions with a precipitation increase in Figure 2b are driven both by enhanced monsoon flow due to an increase in the land-sea differential heating rate (i.e., northern perimeter of the Indian Ocean) and by an increase in the moisture transport as a result of regional circulation changes (i.e., enhanced onshore flow due to a reduced surface roughness as in the northern Amazon basin). This is in contrast to the areas of reduced precipitation that are primarily confined to the equatorial regions where the precipitation change is less influenced by the onshore transport of moisture. In these regions the precipitation reduction is dominated more by local processes such as the weakened flux of moisture from the surface with a reduction in evapotranspiration and complex atmospheric adjustment feedbacks within the atmospheric column and adjacent locations that modify convective activity [Hartmann *et al.*, 2001]. In the tropical forest removal case the atmospheric column appears to be locally self-regulating as it has to adjust how much energy it gets from the Sun. As a result, the local (column) and regional structure respond to the change in the surface forcing. The energy budget approach presented here will help to clarify how and why the precipitation is changing and which atmospheric processes may be responsible; however, it is difficult to separate the contribution from the advection of moisture or moisture convergence from the self-regulation occurring locally within the atmospheric column.

6. Effects of Tropical Forest Removal on the Energy Budget and Climate of Africa

[29] In this example we have focused our detailed energy budget analysis on the tropical forest region of Africa during the SON season. In order to clearly discriminate between the different processes at work, we have identified three main regions within Figure 1 where significant changes are occurring. The three regions progress from west to east and are numbered 1, 2, and 3. Note that part of the third region lies within both the tropical forest and savanna biomes. This is a region partially outside of the deforested region where the climate response does not behave entirely as expected.

[30] We chose the tropical forest region of Africa in the SON season to illustrate this approach for a number of

reasons. First, the tropical forest region of Africa has relatively simple geography with no high mountain ranges adjacent to the tropical forest, like the Andes in South America, or surrounded by the ocean, as with the tropical forest regions on the islands of the Indonesian archipelago. That is, the regional-scale circulation in Africa may not be as complex as in the Amazon basin or subject to the variety of land-sea interactions, as in the Indonesian islands. Second, we chose the SON season for our analysis because this is the onset of the wet season in the model. Third, the energy budget pattern in the African region is well delineated and highlights some of the processes important in the contrasts between the ocean, the deforested region, and regions outside of the deforested areas. Figure 3 shows the control wind vectors at approximately the 900-hPa level and the difference in wind vectors between the tropical forest removal and control simulations. From the wind vectors it is clear that the prevailing flow at this time of the year in our study area is onshore flow from west to east through region 1, then southward flow in region 2, with flow from the east aiding convergence in region 3. Removal of the tropical forests reduces the surface roughness and contributes to the increase in the near-surface wind speed of the onshore and southward flow. It also leads to an increase in surface heating, enhanced convergence, and the import of moisture from the ocean, partly offsetting the reduction in evapotranspiration.

[31] In order to evaluate the climate response to removal of the tropical forests in Africa we analyze the relevant climatological variables averaged over the region of forest removal on the African continent for the SON season and annually (Table 2). Most of the climatological variables for the African zone exhibit a change similar to the pantropical average. Notable exceptions are the specific humidity, precipitation, and total and high-level cloud cover that all have a reduction greater than the pantropical average. This indicates that the African zone may be more reliant on the vegetation's contribution to the atmospheric moisture content and water cycling through convection than for the Amazon or Indonesian regions.

[32] Subregions within the African zone (Figure 1) exhibit striking local behavior in departures from the control run as indicated in Table 3. With respect to temperature and precipitation, region 1 has a slight cooling and reduction in precipitation, region 2 experiences a large warming and severely reduced precipitation, and region 3 has a very small warming and a modest increase in precipitation. We suggest (in section 6.2) that the differing behavior in these subregions is due to changes in the circulation of the middle and lower troposphere that affects the distribution of energy locally and within adjacent regions. A redistribution of energy can contribute to changing the convective precipitation patterns and intensity, ultimately affecting the climate.

6.1. Moist Static Energy Analysis

[33] Figure 4 illustrates the change in dry and moist static energy between the tropical forest removal and control simulations as well as the control simulation for the three regions in the African zone. Note that the lower troposphere is conditionally unstable in all three regions.

[34] With tropical forest removal, region 1 shows a decrease in the dry static energy due to the small surface

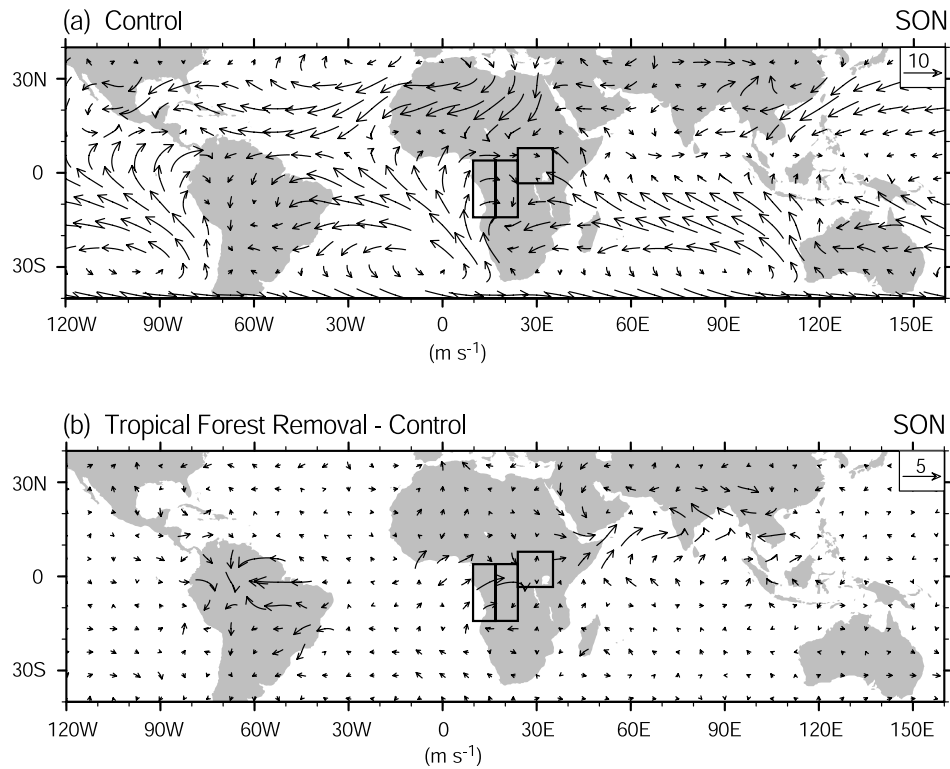


Figure 3. (a) Control simulation winds at level 17 (~ 900 hPa) and (b) change in level 17 winds between tropical forest removal and control simulations for the SON season. Reference vector units are in m s^{-1} . Boxed regions are defined in Figure 1.

cooling and a larger decrease in moist static energy as a result of the drier troposphere. This is due to both a reduction in the surface latent heat flux and precipitation as well as enhanced moisture advection out of the region to the east by the low-level winds along the coast (Figure 3). Here the wind increases over the land but not over the ocean

because of the reduced surface roughness from removal of the vegetation. This causes a divergence in the low-level winds and moisture flux as well as net subsidence that contributes to a reduction in moisture in the region. Region 2 shows an increase in dry static energy caused by a large increase in the near-surface air temperature. There is a large

Table 3. Selected Results From the Tropical Forest Removal Simulation^a

Variable	Region 1		Region 2		Region 3	
	SON	Annual	SON	Annual	SON	Annual
Temperature, K	-0.6 (-0.7)	0.3 (0.5)	2.3 (2.3)	1.4 (1.5)	0.1 (0.2)	0.3 (0.9)
Net radiation, W m^{-2}	-20.2 (-22.4)	-17.2 (-24.7)	-48.2 (-48.2)	-33.3 (-33.3)	-6.0 (-11.3)	-6.0 (-7.4)
Albedo, fraction	0.06 (0.06)	0.05 (0.06)	0.09 (0.09)	0.07 (0.07)	0.00 (0.00)	0.01 (0.01)
Latent heat flux, W m^{-2}	-12.1 (-16.7)	-16.4 (-17.1)	-76.6 (-76.6)	-46.7 (-46.7)	-2.5 (-8.2)	-4.7 (-5.6)
Sensible heat flux, W m^{-2}	-3.2 (-3.2)	2.1 (2.1)	24.6 (24.6)	12.4 (13.6)	-3.6 (-5.7)	-1.6 (-1.6)
Specific humidity, g kg^{-1}	-0.4 (-0.8)	-0.8 (-1.1)	-4.2 (-4.2)	-2.5 (-2.5)	0.0 (-0.1)	-0.2 (-0.4)
Precipitation, mm d^{-1}	-0.7 (-0.9)	-0.7 (-1.1)	-6.0 (-6.0)	-2.8 (-2.8)	1.5 (2.8)	0.5 (0.8)
Total evapotranspiration, mm d^{-1}	-0.7 (-1.0)	-0.9 (-1.0)	-2.6 (-2.6)	-1.6 (-1.6)	-0.1 (-0.3)	-0.2 (-0.2)
Canopy transpiration, mm d^{-1}	-0.6	-1.1	-1.4	-1.7	-0.5	-0.6
Evaporation of canopy-intercepted water, mm d^{-1}	-0.8	-1.0	-2.9	-2.1	-0.9	-0.7
Soil evaporation, mm d^{-1}	0.6 (0.6)	1.2 (1.4)	1.7 (1.7)	2.2 (2.2)	1.2 (2.7)	1.1 (1.4)
PBL height, m	-43.2 (-52.2)	3.1 (6.1)	385.7 (476.2)	100.6 (177.0)	-17.2 (-25.1)	2.5 (14.1)
Total cloud cover, fraction	-0.10 (-0.12)	-0.07 (-0.09)	-0.24 (-0.27)	-0.09 (-0.10)	0.02 (0.03)	0.02 (0.02)
Low-level cloud cover, fraction	0.00 (0.00)	-0.03 (-0.03)	-0.05 (-0.06)	-0.03 (-0.03)	-0.01 (-0.04)	-0.01 (-0.01)
Medium-level cloud cover, fraction	-0.01 (-0.01)	-0.01 (-0.01)	0.02 (0.04)	0.02 (0.03)	0.08 (0.11)	0.04 (0.05)
High-level cloud cover, fraction	-0.13 (-0.15)	-0.07 (-0.09)	-0.26 (-0.29)	-0.10 (-0.11)	0.01 (0.02)	0.02 (0.04)

^aResults are presented as raw differences (tropical forest removal minus control) and are averaged for the SON season and averaged annually for the three regions defined in this study. Statistically significant differences are contained in parentheses and are as defined in Table 2. All variables shown represent surface-level values except the planetary boundary layer height (“PBL height”) and four “cloud cover” variables. Canopy transpiration and evaporation of canopy-intercepted water difference terms are not statistically significant since these terms are constant at zero for the length of the tropical forest removal model run.

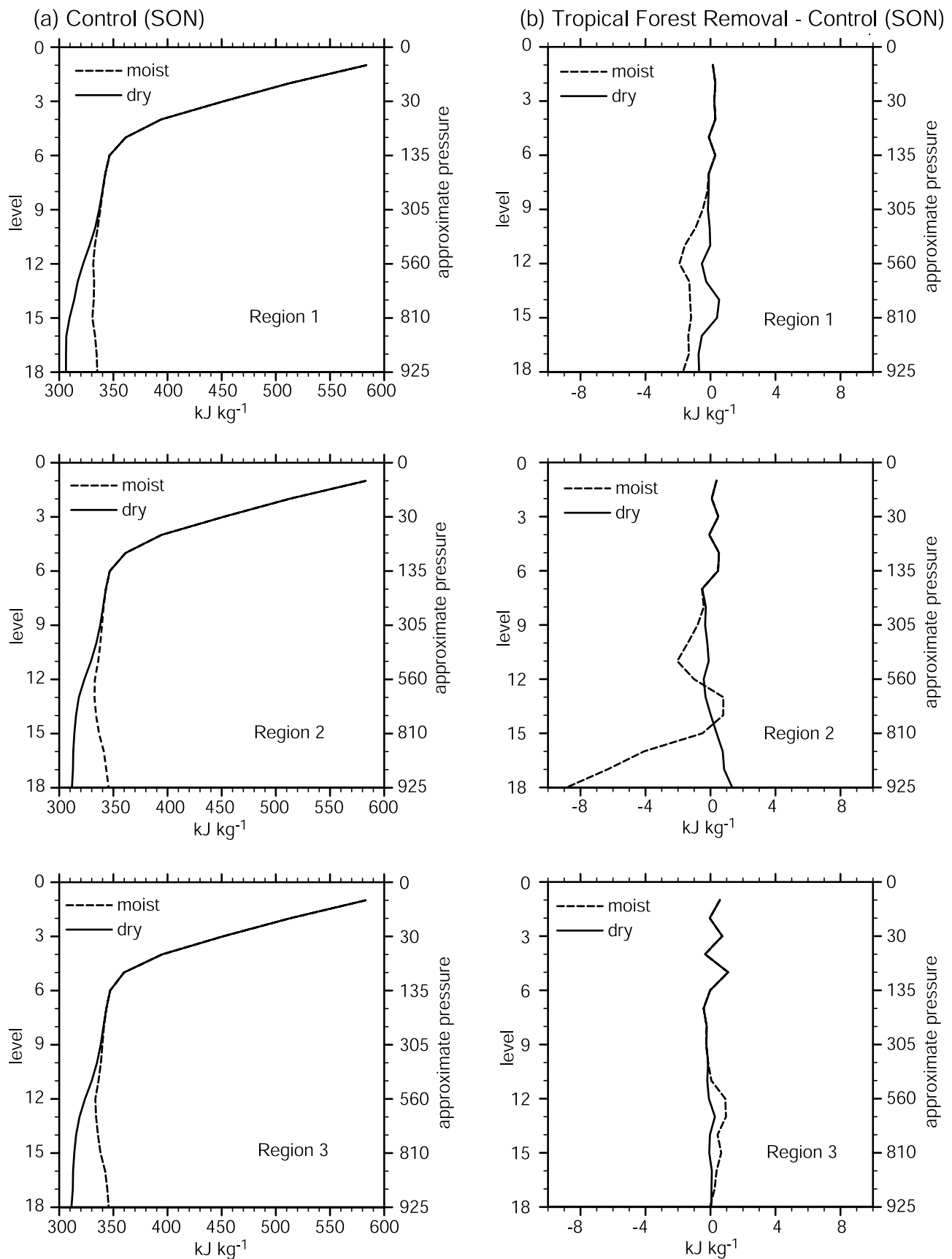


Figure 4. Vertical profile plots of moist static energy (kJ kg^{-1}) for the three African regions of (a) the control simulation and (b) the change between the tropical forest removal and control simulations for the SON season.

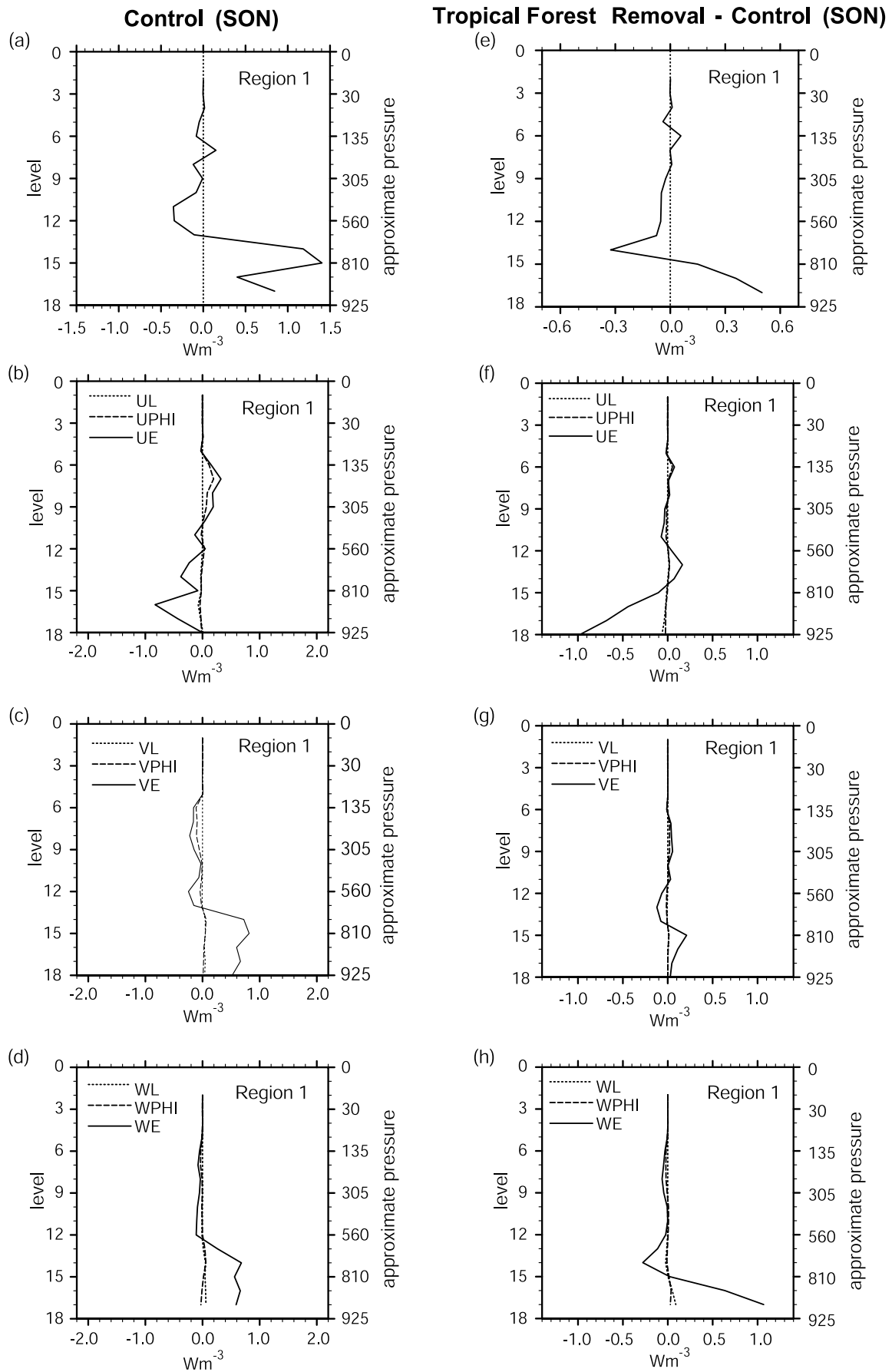


Figure 5

decrease in the moist static energy resulting from a large reduction in the specific humidity of the air from the surface up to level 15 (~ 810 hPa) as well as some advection of moisture to region 3. This is caused by a reduction in the low-level moisture content associated with the weakened flux of moisture from the surface with vegetation removal. There is a small increase in moist static energy at levels 13 (~ 650) and 14 (~ 735 hPa) possibly associated with the advection of moisture from the region to the west or as a result of enhanced condensation. Region 3 shows a small increase in the moist static energy from the surface up to level 11 (~ 470 hPa) that is related to the advection of moisture from the west and the increase in precipitation as noted in Figure 3b and Table 3.

[35] By examining changes in the moist static energy profiles one cannot know the exact mechanism responsible for the change. By examining the profiles it is clear why the energy budget responds as it does near the surface, but changes above the boundary layer are more difficult to explain using this tool. While there might be changes to the advection of energy and moisture from other regions, the exact mechanisms are unclear without analyzing a host of other variables. Therefore analysis of the moist static energy gives a useful view of energy changes but does little to explain how or why the climate changes in the regions.

6.2. Grid Volume Energy Budget Analysis

[36] Owing to the limitations of the moist static energy analysis in determining the influence of the surface forcing on changing the climate, we use our detailed three-dimensional energy budget approach to identify the regions, levels, and mechanisms that influence the climate of a region. Since so much of the climate in the tropical regions is driven by shallow and deep convective processes, we focus on changes in the energy budget to gain insight into modification to these processes and the resulting effect on precipitation. For the tropical forest removal simulation of Africa we describe each of the three regions separately, highlighting the important changes to the energy budget. Furthermore, we identify linkages to the changes in energy between the three regions and offer possible physical mechanisms.

6.2.1. Region 1

[37] Region 1 partially includes the ocean, savanna, and some areas where the tropical forest has been removed (Figure 1). Figure 5 shows the energy budget profiles for region 1. Figures 5a–5d include the control simulation results for the total energy budget and the individual components. Figures 5e–5h are the same energy budget plots but for the change between the tropical forest removal and control simulations. Table 4 lists the percent change in the energy budget for each level in the region.

[38] In the control run the total energy budget has a low-level convergence and upper level divergence of energy. The low-level convergence is due to the meridional and vertical advection of energy, while the upper level divergence is caused by the meridional and vertical divergence of energy. Removal of the tropical forests enhances the low-level convergence of energy through vertical convergence and weakens the convergence or enhances the divergence at higher levels primarily through a reduction in the vertical advection of energy.

[39] The most notable change in the total energy budget for region 1 is in the lower levels (900–800 hPa) where there is a net convergence of energy from enhanced vertical motion. Removal of the tropical forests tends to enhance the already convergent nature of the energy in this region (see Figures 5a and 5e). Zonally, there is a large divergence of energy initiated by tropical forest removal (see Figures 5b and 5f). The zonal divergence is primarily associated with the reduced surface roughness that enhances the advection of internal energy out of the region. Therefore the convergence in energy at these levels is driven primarily by vertical convergence as dictated by the changes to the vertical motion (ω). Some of the increase in energy at levels 17–15 is transported eastward to the central region. Above level 15, upward vertical motion weakens, and there is an enhanced divergence of energy in the vertical direction as much of the energy is instead advected eastward. Although a true energy budget value is not calculated at level 18, it is clear from the change in the zonal energy budget components and the enhanced vertical motion at the surface that energy is propagated above (to levels 17–15) and also eastward to region 2.

[40] The 200-hPa level (between levels 8 and 7) typically reflects the approximate height where deep convective outflow occurs in the model. In the control simulation this zone is characterized by zonal convergence and meridional and vertical divergence of energy. In the tropical forest removal simulation, there is little change in the total energy budget at this level with a small enhancement of the vertical divergence of energy and a slight meridional convergence of energy. The small changes in the total energy at these levels indicates that the surface forcing has a small effect on the convection and the corresponding precipitation in this region.

6.2.2. Region 2

[41] Region 2 is unique in that all the cells included in the region have had the tropical forest removed (see Figure 1). As a result, it is expected that there will be a large change in the energy budget above and around the area of surface forcing. Figure 6 shows the energy budget profiles for region 2. Table 4 lists the percent change in the energy budget for each level in the region.

Figure 5. Vertical profile plots for region 1 of (a) the control total energy budget, (b–d) the control individual energy budget components, (e) the change in the total energy budget, and (f–h) the change in the individual components between the tropical forest removal and control simulations for the SON season. Positive values of UE, UPHI, UL (VE, VPHI, VL and WE, WPHI, WL) represent the convergence of the internal (E), geopotential (PHI), and latent (L) energy fluxes in the zonal (U) (meridional (V) and vertical (W)) direction, respectively. Dotted vertical line in total energy budget plots is a zero reference line.

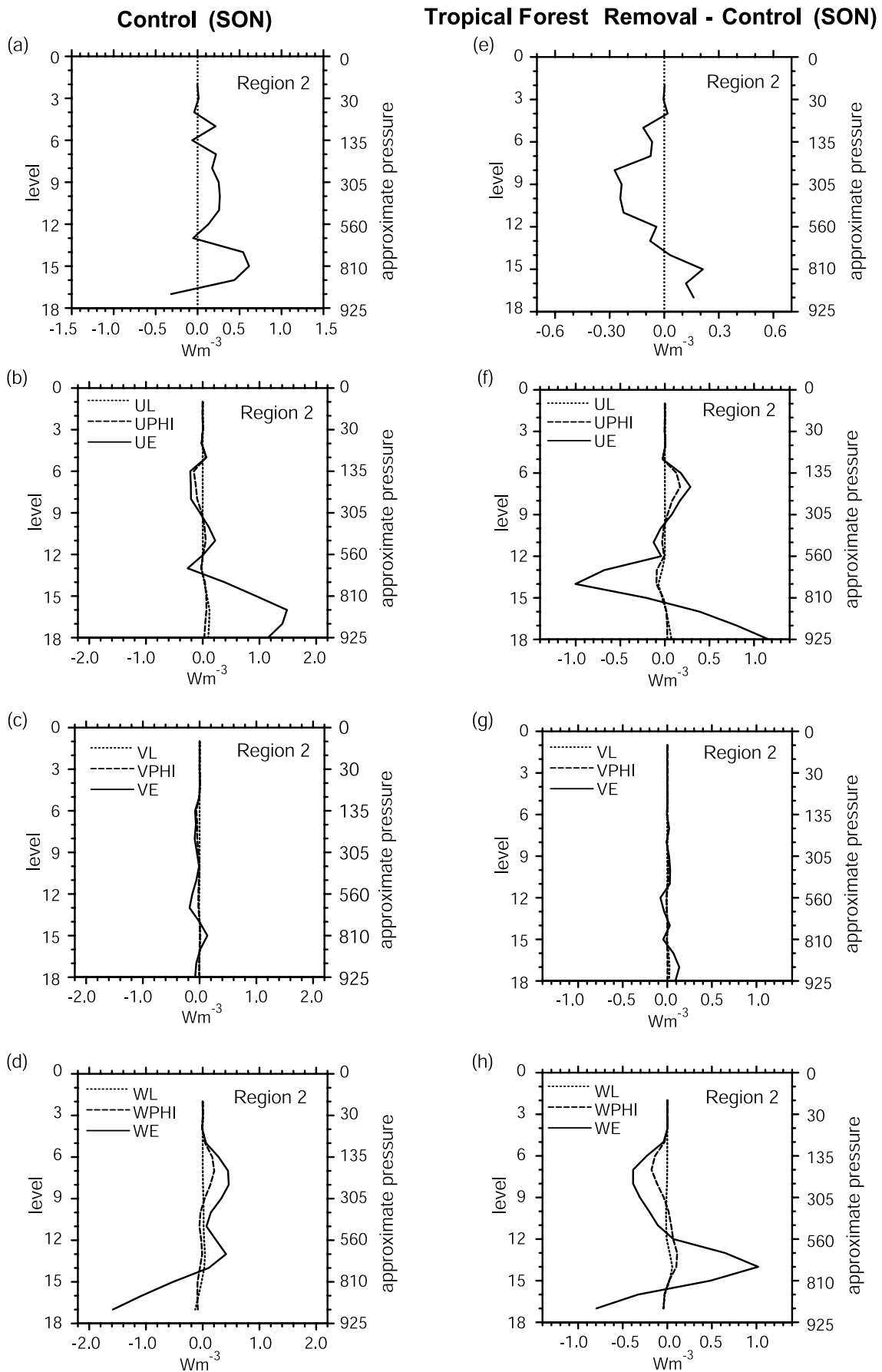


Figure 6. Same as Figure 5 except results presented for region 2.

Table 4. Percent Change in the Total Energy Budget (Tropical Forest Removal Minus Control) for Each of Three Regions Described in This Study^a

Level	Region 1	Region 2	Region 3
1	na	na	na
2	57.9	-62.0	113.8
3	58.4	-33.0	121.0
4	70.1	-45.5	172.5
5	83.0	-53.8	23.5
6	-69.7	103.3	-18.3
7	-1.1	-34.1	-4.4
8	-6.7	-157.7	61.5
9	310.0	-93.0	5.7
10	57.6	-91.0	91.2
11	14.2	-87.5	47.5
12	15.2	-33.1	-51.9
13	70.1	146.1	79.6
14	-27.5	5.9	-0.9
15	10.6	34.6	-35.9
16	89.6	27.2	119.9
17	59.3	-51.1	73.2
18	na	na	na

^aData presented for the 18 vertical levels in the atmospheric general circulation model during the SON season; “na,” not applicable.

[42] In region 2 the control run total energy budget shows a divergence of energy at the lowest level and convergence or no change in energy at higher levels. The divergence at the lowest level is due to strong vertical divergence of energy from enhanced vertical motion at the surface. Convergence in energy at higher levels is due to both zonal and vertical convergence. In the tropical forest removal simulation, there is weakened divergence at the lowest level caused by a large zonal convergence of energy from region 1. Levels 16–14 (~865–735 hPa) are convergent in region 2, and this is associated with the strong divergence noted at levels 17–15 (~905–810 hPa) in region 1. At higher levels, there is weakened convergence of energy caused both by weakened zonal and vertical convergence of energy.

[43] The convergence of energy in the zonal direction at low levels is compensated for by the increased divergence in the vertical direction. This is due to both the enhanced vertical motion from the warmer land surface and the increase in energy advected from region 1. Once above level 16 (~865 hPa), vertical motion weakens and the convergence of energy is transported zonally and vertically into the region. Finally, the surface energy zonal component (level 18) shows a doubling in the convergence of energy due to the strong divergence from region 1. Some of this energy is advected eastward to region 3, while some is transported upward because of the increase in vertical motion from the warmer land surface.

[44] From levels 13 to 4 (~650 to ~65 hPa), there is a decrease in the total energy budget caused by both the large zonal divergence (from levels 15 to 12) and the vertical divergence from levels 12 to 4 (~560 to ~65 hPa). The large zonal divergence and vertical convergence centered on level 14 (~735 hPa) transports energy to the east, but not upward, and is associated with enhanced shallow and drier convective overturning. Much of the energy that is transported eastward (some to region 3) at this level is then unavailable for transport vertically to higher levels in the atmosphere. The enhanced divergence at level 14 prevents the transport of energy to higher levels in the atmosphere,

limits the strength of deep convection, and contributes to the large reduction in precipitation in the region.

6.2.3. Region 3

[45] Region 3 is also unique in that it partially contains a region where the tropical forests have been removed and a region with savanna vegetation (Figure 1). It is here where the changes in the atmospheric energy budget in the other two regions affect the climate through changes in the circulation and strength of convective precipitation. Figure 7 shows the energy budget profiles for Region 3. Table 4 lists the percent change in the energy budget for each level in the region.

[46] In the control run, there is a convergence of total energy throughout the atmospheric column except at level 17. The convergence is due primarily to the zonal and vertical convergence of energy. In the tropical forest removal simulation, there is enhanced convergence of energy at all levels except level 15 (~810 hPa) where there is weakened convergence. In contrast to regions 1 and 2 where there is an increase in low-level energy and a decrease at higher levels, the energy budget profile for region 3 shows an increase at almost all levels (level 15 is the exception). Region 3 also differs from the other regions in that shallow convection (defined by weakened convergence at level 15) decreases in favor of deep convection, while in regions 1 and 2 the opposite occurs with deep convection weakened and shallow convection enhanced (see Figures 5 and 6).

[47] At level 15, there is weakened convergence of energy with tropical forest removal that implies a reduction in the shallow convective overturning as energy is instead transported to higher levels where it is used to fuel deep convection. At the surface (level 18), there is enhancement in the zonal convergence of energy contributed from the regions to the west (i.e., region 2); however, this is offset by the divergence meridionally out of the area and vertically to higher levels. There is almost no change in the convergence of total energy at level 14 (~735 hPa), although there is an increase in the divergence of energy that makes its way into region 3 as noted by the small increase in the zonal convergence of energy. This increase in zonal energy is offset by the weakened vertical convergence (to divergence) that helps to transport energy to higher levels where it can be used to drive deep tropical convection. Therefore, although there is a net influx of zonal energy from region 2, the vertical divergence of energy to higher levels causes little change in the energy at that level. From levels 13 to 6 (~650 to ~135 hPa) (not including level 12), there is enhanced convergence in the vertical direction as the energy from lower levels is transported to higher levels where it is used to drive deep convection. There is also a weakening of meridional divergence at level 13 (~650 hPa), and this weakening is a further indicator of the weakening of shallow convection in favor of the more energy intensive deep convective processes.

[48] Maximum tropical outflow occurs at ~200 hPa (levels 8 and 7) and is coincident with the large increases in energy transported from below. This is identified by the enhanced vertical convergence, weakened zonal divergence, and enhanced meridional divergence at these levels. Figure 8 illustrates the total energy budget at level 8 (~240 hPa) for the control run and the change in the

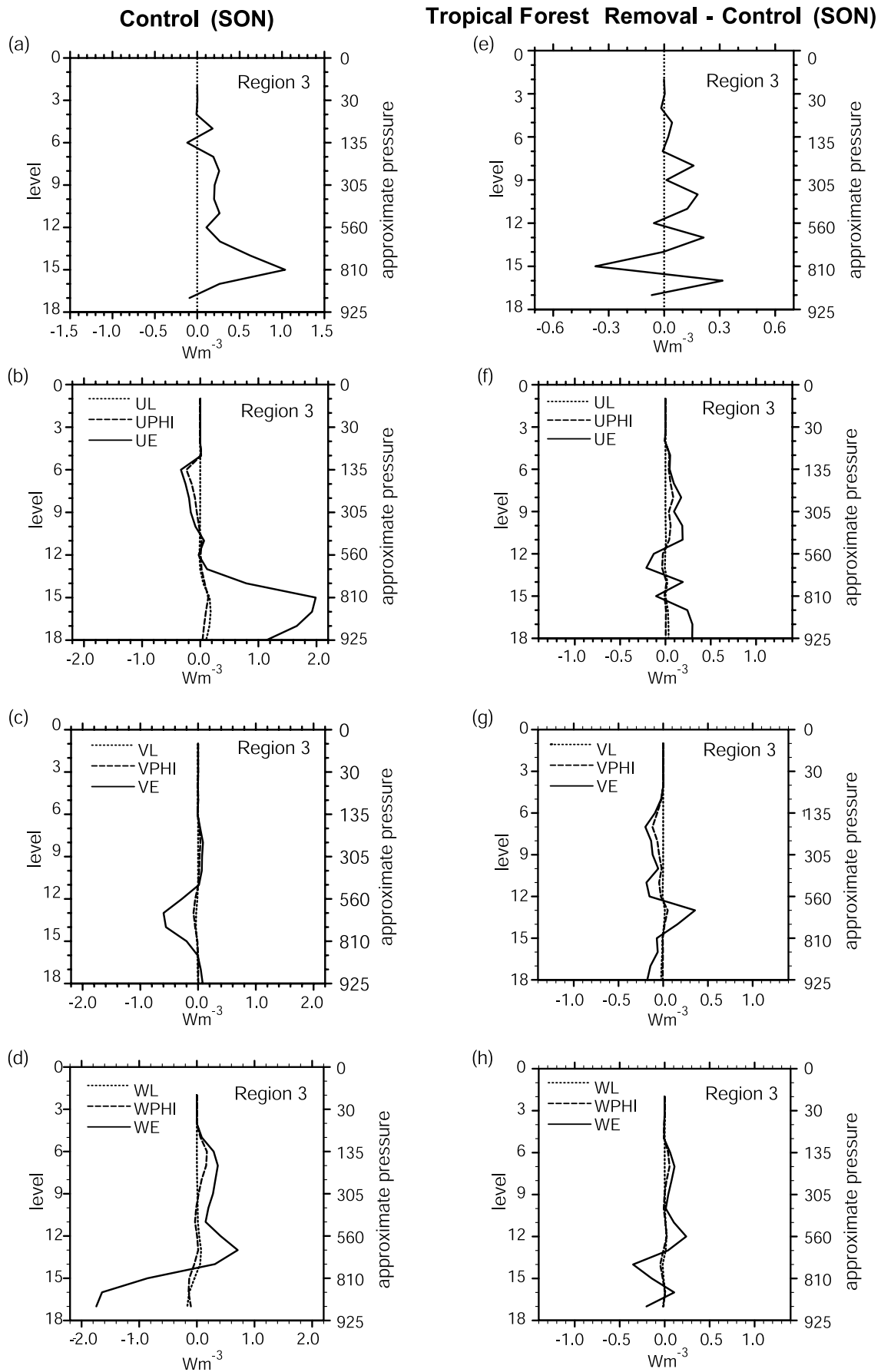


Figure 7. Same as Figure 5 except results presented for region 3.

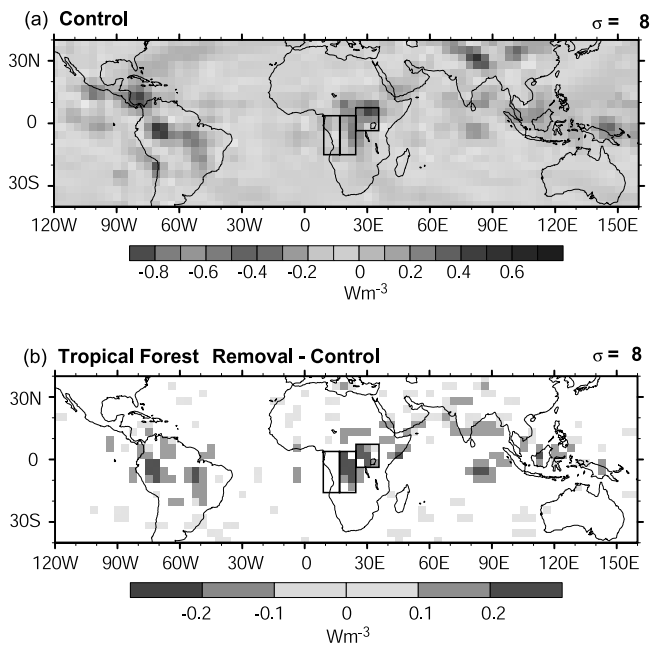


Figure 8. Tropical distribution of SON changes in total energy budget (W m^{-3}) at level 8 (~ 240 hPa) for (a) control simulation and (b) the difference (tropical forest removal minus control) with significance as defined in Figure 2. See color version of this figure at back of this issue.

total energy budget between the deforestation and control simulations. From Figure 8 it can be seen that region 2 has a large loss of energy (weakened vertical convergence) associated with reduced deep tropical convection. Region 3 has a large increase in energy (enhanced vertical convergence) associated with an increase in deep tropical convection. If Figure 8 is compared to Figure 2, the change in precipitation with tropical forest removal, it is evident that regions of increased precipitation are aligned with regions of increased energy and regions with a precipitation decrease are associated with regions of decreased energy at level 8. The control run results indicate that these are regions that normally have a large amount of energy at that level. Therefore changes in the biophysical processes at the surface can have a large influence on the energy budget of the atmosphere and the climate, even at high levels.

[49] To further illustrate the change in the energy budget profile over a region of increased precipitation, Figure 9 represents the profile over a region of increased precipitation in the northern Amazon basin (see Figure 2b). This is a region where the annual precipitation increases by $\sim 50\%$ (from 6.3 to 9.5 mm d^{-1}). Figure 9 shows the energy budget profiles for the northern Amazon basin.

[50] The change in the total energy budget (Figure 9e) shows a net increase in energy for all levels except level 14 (~ 735 hPa) where tropical forest removal causes a loss of energy while in the control run there is a convergence of energy. The low-level convergence of energy is related to the increase in zonal energy advected from the east and trapped by the Andes mountain range to the west. Meridional divergence is enhanced as the low-level winds increase with the reduced surface roughness, resulting in

energy being advected south of the region of increased precipitation. Finally, there is enhanced vertical divergence at low levels (15 and 14) as shallow convective overturning is reduced in favor of deep convection as evidenced by the increase in the vertical convergence of energy above level 14.

7. Summary of the Energy Budget Analysis

[51] Figure 10 summarizes the relevant energy linkages between the three regions and the primary mechanisms whereby upper level energy in region 3 contributes to enhancing deep convection and increasing precipitation. In region 1, there is a loss of energy at the surface associated with the increase in low-level winds advecting warm air to the east. Near-surface vertical motion is also enhanced, and this contributes to enhancing the convergence of energy at low levels (~ 905 – 810 hPa). At level 16 (~ 865 hPa), there is enhanced divergence of energy out of the region to the east. This results in less energy available for driving deep convection at higher levels. Above level 14 (~ 735 hPa), there is a loss of energy imported from below (enhanced vertical divergence).

[52] In region 2, there is enhanced convergence of energy at the surface related to the advection of energy out of region 1. Enhanced vertical motion at the surface transports some of this energy aloft, where it converges with energy coming from region 1 at level 16 (~ 865 hPa). Enhanced vertical convergence at levels 16–14 (~ 865 – 735 hPa) combined with zonal convergence of energy from the west creates a pocket of enhanced convergence of energy. At level 14 (~ 735 hPa), energy is advected east from region 2 as zonal convergence switches to zonal divergence in the tropical forest removal simulation. The transport of energy eastward combined with weakened vertical motion weakens the convergence of energy vertically above level 14. It is this large reduction in energy at higher levels that contributes to a significant reduction in deep convective precipitation in favor of the less energy intensive shallow convective overturning.

[53] In region 3, there is an increase in energy advected from region 2 at the surface. The vertical motion is unchanged, although it enhances once away from the surface. There is enhanced convergence of energy zonally from region 2 at level 14 (~ 735 hPa) along with weakened convergence vertically associated with enhanced vertical motion. The increase in energy and increased vertical motion transports energy to high levels where it is used to fuel deep convection. In contrast to region 2, results from region 3 show that deep convection is favored over shallow convection as there is adequate energy available. Over the deforested regions (e.g., region 2), there is not adequate energy for driving deep convection, so what energy is available is instead used for shallow convection.

[54] In summary, changes in the advection of energy at the surface combined with vertical advection of energy to higher levels aid energy transport to other regions where it can be used in convective precipitation processes. In region 1, there is a convergence of energy at levels 17–15 that is carried to the central region at level 16 (~ 865 hPa). In region 2, energy from the surface and region 1 combines to form an area of energy convergence

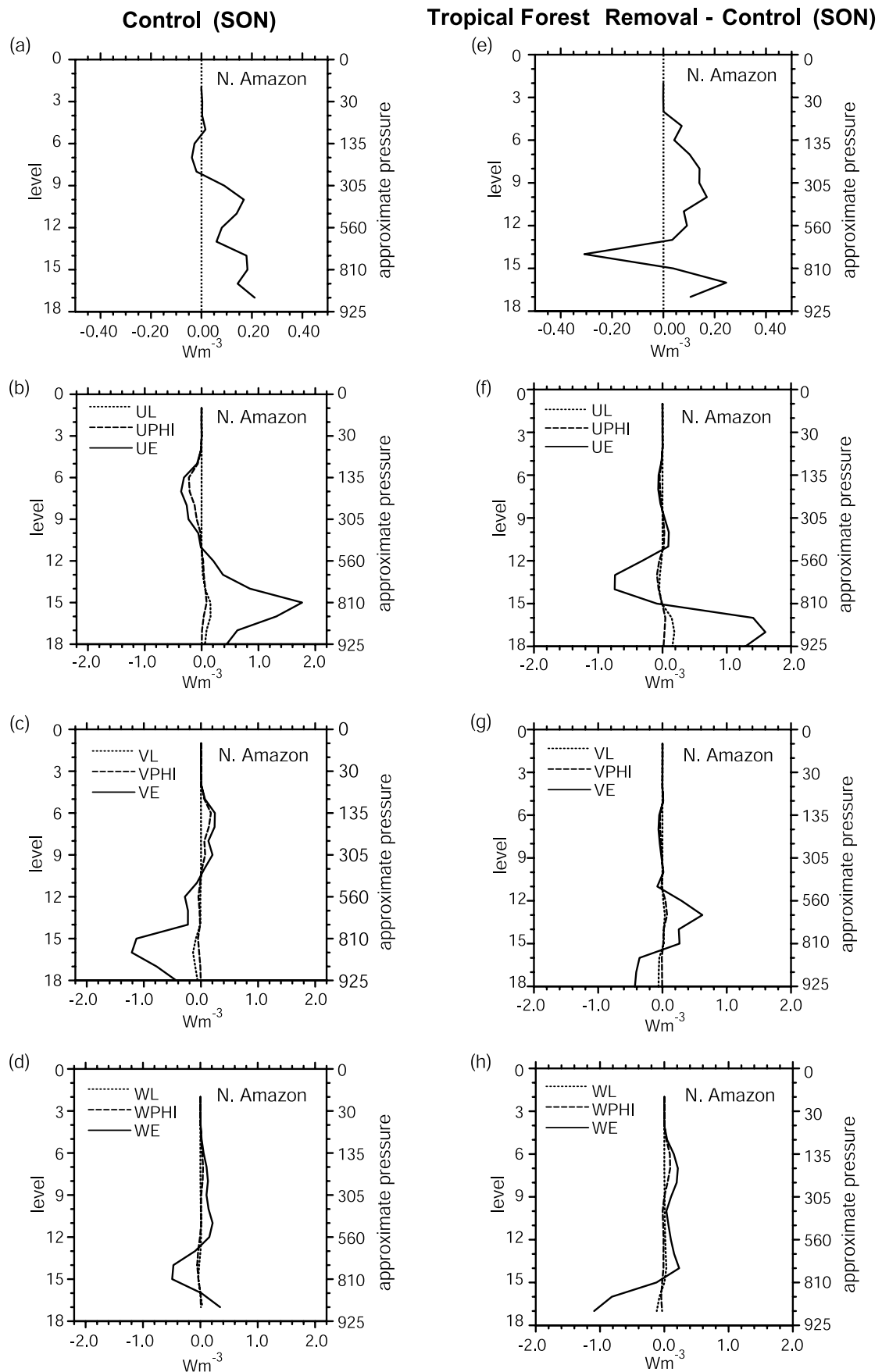


Figure 9. Same as Figure 5 except results presented for a region in the northern Amazon basin of high precipitation (see Figure 2b).

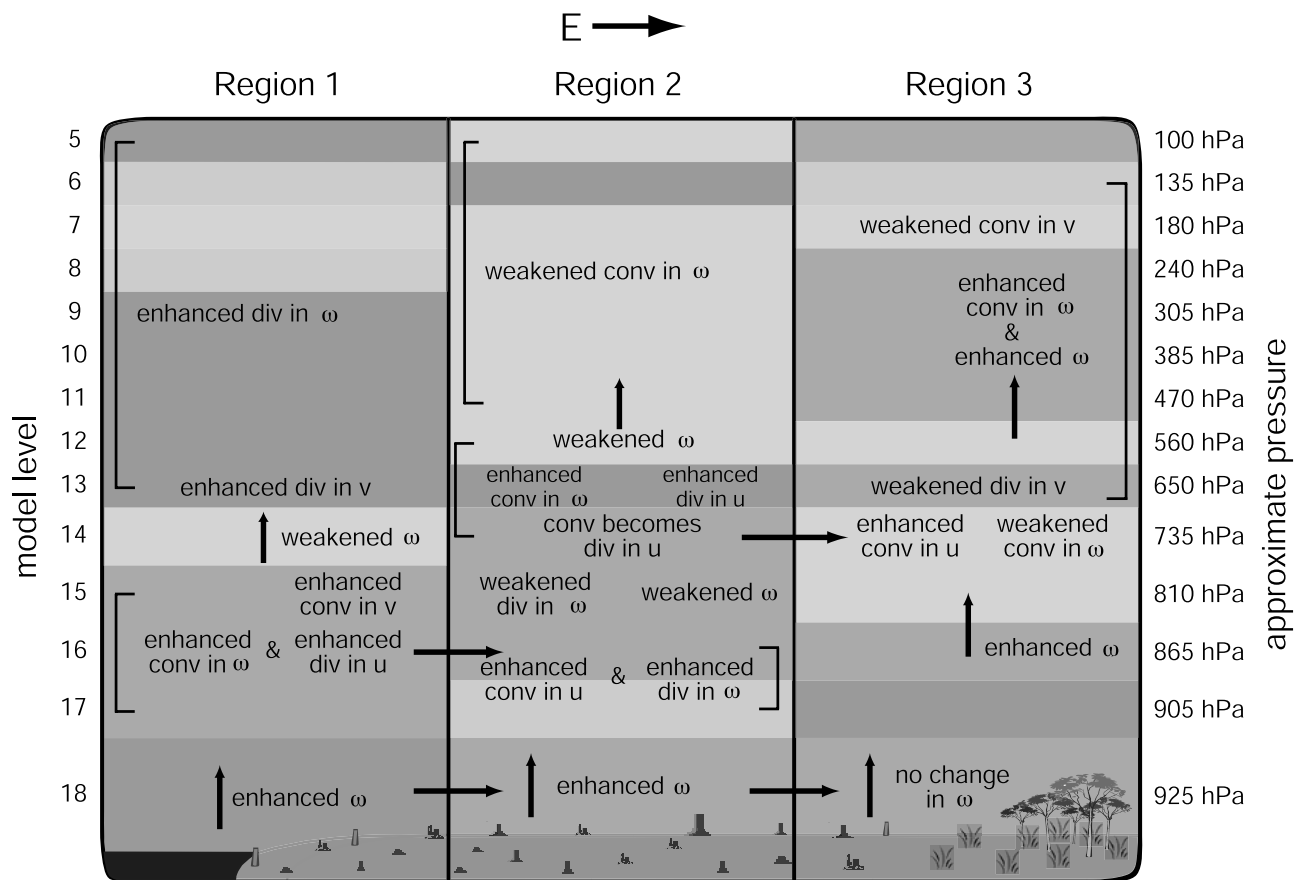


Figure 10. Qualitative summary illustrating the important changes in the energy budget between the three regions as a result of tropical forest removal. Dark blue regions depict areas of enhanced energy divergence (loss), while light blue regions depict areas of weakened energy divergence (gain). Dark pink regions depict areas of enhanced energy convergence (gain), while light pink regions depict areas of weakened energy convergence (loss). The letters “*u*,” “*v*,” and “ ω ” refer to zonal, meridional, and vertical directions of energy convergence or divergence, respectively. East is to the right. See color version of this figure at back of this issue.

at levels 16–14 (~ 865 – 735 hPa). This energy is then transferred to region 3 at level 14 (~ 735 hPa). Energy convergence at most levels of region 3 comes from the transfer of energy from region 2 at level 14 as well as from the surface energy that was advected from the west. Enhanced vertical motion increases the convergence of energy throughout the atmospheric column to levels where deep convective processes are important.

8. Summary and Conclusions

[55] In tropical regions the surface exchange of water and energy plays a vital role in maintaining the climate system. The partitioning and distribution of energy have a significant influence by modifying near-surface climatic variables such as temperature and precipitation. Shallow and deep tropical convection are also important processes in tropical climatology as they provide the mechanisms for the transfer of energy between the surface, the atmosphere, and higher latitudes through atmospheric teleconnections. The land surface has a strong influence on tropical convection through its role in the exchange of energy and water with the atmosphere. As a result, changes in land surface

properties can directly influence the positioning and intensity of tropical convection.

[56] In this paper we have described a new method to explore how land use and land cover change can influence the climate at the regional scale. Using a coupled atmosphere-biosphere model, we examine the influence that tropical forest removal can have on the regional climate by carefully accounting for the changes in the three-dimensional atmospheric energy budget. We have illustrated the mechanisms that act to change the energy budget and to alter the climate in regions that may be removed from the surface forcing or in the same region where it exhibits uncharacteristic behavior.

[57] The energy budget approach described in this paper can be used to synthesize different variables and atmospheric processes. Instead of tracking a multitude of variables, one can instead examine the total energy budget (and its individual components) in order to determine the basic climatic mechanisms at work. Traditionally, studies have focused on the use of moist static energy as a diagnostic for understanding how and why the climate changes. However, this approach does not take into account the important role of advection and radiative processes in the atmosphere.

Changes in the moist static energy may be due to advection from other regions or from the surface, and a more detailed analysis must be performed to understand which processes are important.

[58] While this three-dimensional energy budget method can be useful in atmosphere-biosphere studies, we acknowledge that there are limitations to the present study. First, changes in the energy content of the tropical atmosphere as modeled with CCM3-IBIS are based on the accuracy of the CCM3 convective parameterization scheme. Sensitivity of the model to outside parameters (i.e., flux from the land surface) and the boundary layer thermodynamics can have a considerable impact on the position and intensity of tropical convection. Second, there are limitations with using static vegetation (vegetation structure and biogeography not allowed to change in response to the climate). Certainly, changes to the land surface from tropical forest removal will not maintain a desert environment, but rather different vegetation may eventually replace the forest and interact with the climate differently. Third, the model parameterization of the biosphere can have a strong influence on the climate through such factors as the rate of evapotranspiration, the albedo, and the roughness length. It is clear that the choice of parameterization of these processes can have a significant effect on the climate. Fourth, we acknowledge that the use of fixed sea surface temperatures prevents us from capturing the important atmosphere-ocean feedbacks that play a role in the tropics; however, it is necessary for isolating the influence of only the vegetation changes on the climate. More realistic studies that address observed land use and land cover change should employ a model with interactive sea surface temperatures. Finally, to have better confidence in the results of future studies using this approach, a set of ensemble simulations should be performed so that multiple realizations can provide a better estimate of the statistically significant changes to the regional atmospheric energy budget caused by land use and land cover change.

[59] **Acknowledgment.** The authors thank Chad Monfreda for use of his "Lost Land" data set that allowed us to determine the current loss of potential vegetation in the tropics as defined in IBIS.

References

- Amthor, J. S. (1984), The role of maintenance respiration in plant growth, *Plant Cell Environ.*, *7*, 561–569.
- Baidya Roy, S., and R. Avissar (2002), Impact of land use/land cover change on regional hydrometeorology in Amazonia, *J. Geophys. Res.*, *107*(D20), 8037, doi:10.1029/2000JD000266.
- Charney, J. G. (1975), Dynamics of deserts and droughts in the Sahel, *Q. J. R. Meteorol. Soc.*, *101*, 193–202.
- Chase, T. N., R. A. Pielke, T. G. F. Kittel, R. R. Nemani, and S. W. Running (2000), Simulated impacts of historical land cover changes on global climate in northern winter, *Clim. Dyn.*, *16*, 93–105.
- Collatz, G. J., J. T. Ball, C. Grivet, and J. A. Berry (1991), Physiological and environmental regulation of stomatal conductance, photosynthesis and transpiration: A model that includes a laminar boundary layer, *Agric. For. Meteorol.*, *53*, 107–136.
- Collatz, G. J., M. Ribas-Carbo, and J. A. Berry (1992), Coupled photosynthesis-stomatal conductance model for leaves of C₄ plants, *Aust. J. Plant Physiol.*, *19*, 519–538.
- Costa, M. H., and J. A. Foley (2000), Combined effects of deforestation and doubled atmospheric CO₂ concentrations on the climate of Amazonia, *J. Clim.*, *13*, 18–34.
- Delire, C., S. Levis, G. B. Bonan, J. A. Foley, M. T. Coe, and S. Vavrus (2002), Comparison of the climate simulated by the CCM3 coupled to two different land-surface models, *Clim. Dyn.*, *19*, 657–669.
- Dickinson, R. E., and A. Henderson-Sellers (1988), Modelling tropical deforestation: A study of GCM land-surface parameterizations, *Q. J. R. Meteorol. Soc.*, *114*, 439–462.
- Dickinson, R. E., and P. Kennedy (1992), Impacts on regional climate of Amazon deforestation, *Geophys. Res. Lett.*, *19*, 1947–1950.
- Eltahir, E. A. B. (1996), Role of vegetation in sustaining large-scale atmospheric circulations in the tropics, *J. Geophys. Res.*, *101*, 4255–4268.
- Eltahir, E. A. B., and R. L. Bras (1993), On the response of the tropical atmosphere to large-scale deforestation, *Q. J. R. Meteorol. Soc.*, *119*, 779–793.
- Farquhar, G. D., S. von Caemmerer, and J. A. Berry (1980), A biochemical model of photosynthetic CO₂ assimilation in leaves of C₃ species, *Planta*, *149*, 78–90.
- Foley, J. A., I. C. Prentice, N. Ramankutty, S. Levis, D. Pollard, S. Sitch, and A. Haxeltine (1996), An integrated biosphere model of land surface processes, terrestrial carbon balance, and vegetation dynamics, *Global Biogeochem. Cycles*, *10*, 603–628.
- Food and Agricultural Organization (2001), Forest resources assessment 2000, report, Rome.
- Gill, A. E. (1982), *Atmosphere-Ocean Dynamics*, 662 pp., Academic, San Diego, Calif.
- Hack, J. J., J. T. Kiehl, and J. W. Hurrell (1998), The hydrologic and thermodynamic characteristics of the NCAR CCM3, *J. Clim.*, *11*, 1179–1206.
- Hartmann, D. L., L. A. Moy, and Q. Fu (2001), Tropical convection and the energy balance at the top of the atmosphere, *J. Clim.*, *14*, 4495–4511.
- Henderson-Sellers, A., R. E. Dickinson, T. B. Durbridge, P. J. Kennedy, K. McGuffie, and A. J. Pitman (1993), Tropical deforestation: Modeling local- to regional-scale climate change, *J. Geophys. Res.*, *98*, 7289–7315.
- International Geosphere-Biosphere Programme Data and Information System (1999), Global soil data task: Spatial database of soil properties, <http://www.daac.ornl.gov>, Oak Ridge Natl. Lab., Oak Ridge, Tenn.
- James, I. N. (1994), *Introduction to Circulating Atmospheres*, 422 pp., Cambridge Univ. Press, New York.
- Kiehl, J. T., J. J. Hack, G. B. Bonan, B. A. Boville, D. L. Williamson, and P. J. Rasch (1998), The National Center for Atmospheric Research Community Climate Model: CCM3, *J. Clim.*, *11*, 1131–1149.
- Kucharik, C. J., J. A. Foley, C. Delire, V. A. Fisher, M. T. Coe, J. D. Lenters, C. Young-Molling, N. Ramankutty, J. M. Norman, and S. T. Gower (2000), Testing the performance of a Dynamic Global Ecosystem Model: Water balance, carbon balance, and vegetation structure, *Global Biogeochem. Cycles*, *14*, 795–825.
- Lean, J., and P. R. Rowntree (1993), A GCM simulation of the impact of Amazonian deforestation on climate using an improved canopy representation, *Q. J. R. Meteorol. Soc.*, *119*, 509–530.
- Lean, J., and D. A. Warrilow (1989), Simulation of the regional climatic impact of Amazon deforestation, *Nature*, *342*, 411–413.
- Marland, G., et al. (2003), The climatic impacts of land surface change and carbon management, and the implications for climate-change mitigation policy, *Clim. Policy*, *3*, 149–157.
- Nobre, C. A., P. J. Sellers, and J. Shukla (1991), Amazonian deforestation and regional climate change, *J. Clim.*, *4*, 957–988.
- Pielke, R. A. (2001), Influence of the spatial distribution of vegetation and soils on the prediction of cumulus convective rainfall, *Rev. Geophys.*, *39*, 151–177.
- Pielke, R. A., G. Marland, R. A. Betts, T. N. Chase, J. L. Eastman, J. O. Niles, D. D. S. Niyogi, and S. W. Running (2002), The influence of land-use change and landscape dynamics on the climate system: Relevance to climate-change policy beyond the radiative effect of greenhouse gases, *Philos. Trans. R. Soc. London, Ser. A*, *360*, 1705–1719.
- Polcher, J. (1995), Sensitivity of tropical convection to land-surface processes, *J. Atmos. Sci.*, *52*, 3143–3161.
- Polcher, J., and K. Laval (1994), The impact of African and Amazonian deforestation on tropical climate, *J. Hydrol.*, *155*, 389–405.
- Ramankutty, N., and J. A. Foley (1999), Estimating historical changes in global land cover: Croplands from 1700 to 1992, *Global Biogeochem. Cycles*, *13*, 997–1027.
- Snyder, P. K., C. Delire, and J. A. Foley (2004), Evaluating the influence of different vegetation biomes on the global climate, *Clim. Dyn.*, *23*, 279–302, doi:10.1007/s00382-004-0430-0.
- Sud, Y. C., J. Shukla, and Y. Mintz (1988), Influence of land surface-roughness on atmospheric circulation and precipitation—A sensitivity study with a general-circulation model, *J. Appl. Meteorol.*, *27*, 1036–1054.
- Sud, Y. C., G. K. Walker, J. H. Kim, G. E. Liston, P. J. Sellers, and W. K. M. Lau (1996), Biogeophysical consequences of a tropical deforestation scenario: A GCM simulation study, *J. Clim.*, *9*, 3225–3247.
- Wang, G. L., and E. A. B. Eltahir (2000a), Biosphere-atmosphere interactions over West Africa. I: Development and validation of a coupled dynamic model, *Q. J. R. Meteorol. Soc.*, *126*, 1239–1260.

- Wang, G. L., and E. A. B. Eltahir (2000b), Biosphere-atmosphere interactions over West Africa. II: Multiple climate equilibria, *Q. J. R. Meteorol. Soc.*, *126*, 1261–1280.
- Wang, G. L., and E. A. B. Eltahir (2000c), Ecosystem dynamics and the Sahel drought, *Geophys. Res. Lett.*, *27*, 795–798.
- Werth, D., and R. Avissar (2002), The local and global effects of Amazon deforestation, *J. Geophys. Res.*, *107*(D20), 8087, doi:10.1029/2001JD000717.
- Xue, Y. K., and J. Shukla (1993), The influence of land-surface properties on Sahel climate. 1. Desertification, *J. Clim.*, *6*, 2232–2245.
- Zeng, N., R. E. Dickinson, and X. B. Zeng (1996), Climatic impact of Amazon deforestation—A mechanistic model study, *J. Clim.*, *9*, 859–883.
- Zhang, H., K. McGuffie, and A. Henderson-Sellers (1996), Impacts of tropical deforestation. Part II: The role of large-scale dynamics, *J. Clim.*, *9*, 2498–2521.
- Zhao, M., A. J. Pitman, and T. Chase (2001), The impact of land cover change on the atmospheric circulation, *Clim. Dyn.*, *17*, 467–477.

C. Delire, Institut des Sciences de l'Evolution (UMR CNRS 5554), Université Montpellier II - pl. E. Bataillon, case postale 61, F-34095, Montpellier cedex 05, France.

J. A. Foley and P. K. Snyder, Center for Sustainability and the Global Environment, Nelson Institute for Environmental Studies, University of Wisconsin-Madison, 1710 University Avenue, Madison, WI 53726, USA. (pksnyder@wisc.edu)

M. H. Hitchman, Department of Atmospheric and Oceanic Sciences, University of Wisconsin-Madison, 1225 West Dayton Street, Madison, WI 53706, USA.

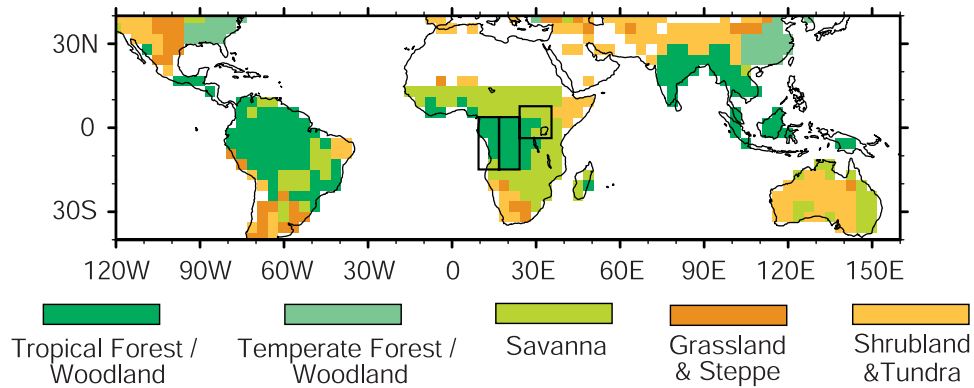


Figure 1. Tropical distribution of the five potential vegetation biomes defined in this study at T31 spatial resolution. Each biome includes one or more vegetation types as defined in the IBIS land surface model. Boxed areas in Africa represent averaging areas and are identified from west to east as regions 1, 2, and 3.

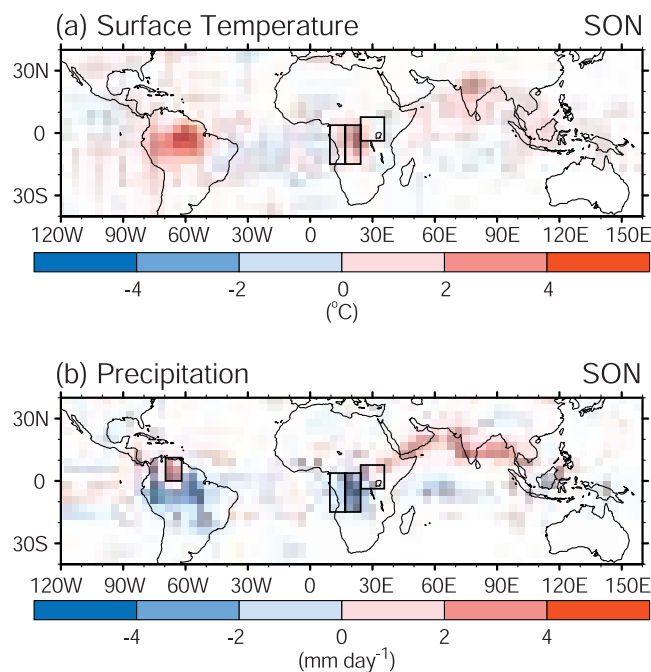


Figure 2. Tropical distribution of September–October–November (SON) changes in (a) surface temperature ($^{\circ}\text{C}$) and (b) precipitation (mm day^{-1}) due to tropical forest removal. Differences (tropical forest removal minus control) are shown only for cells significant at the 95% significance level using a two-sided Student's t test. Boxed regions in Africa are defined in Figure 1. The boxed region in South America on the precipitation map represents the area referenced in Figure 9.

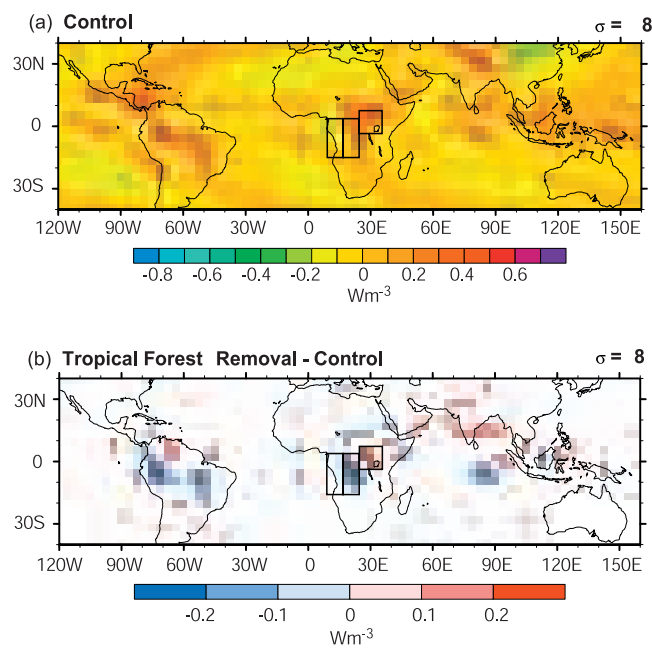


Figure 8. Tropical distribution of SON changes in total energy budget ($W m^{-3}$) at level 8 (~ 240 hPa) for (a) control simulation and (b) the difference (tropical forest removal minus control) with significance as defined in Figure 2.

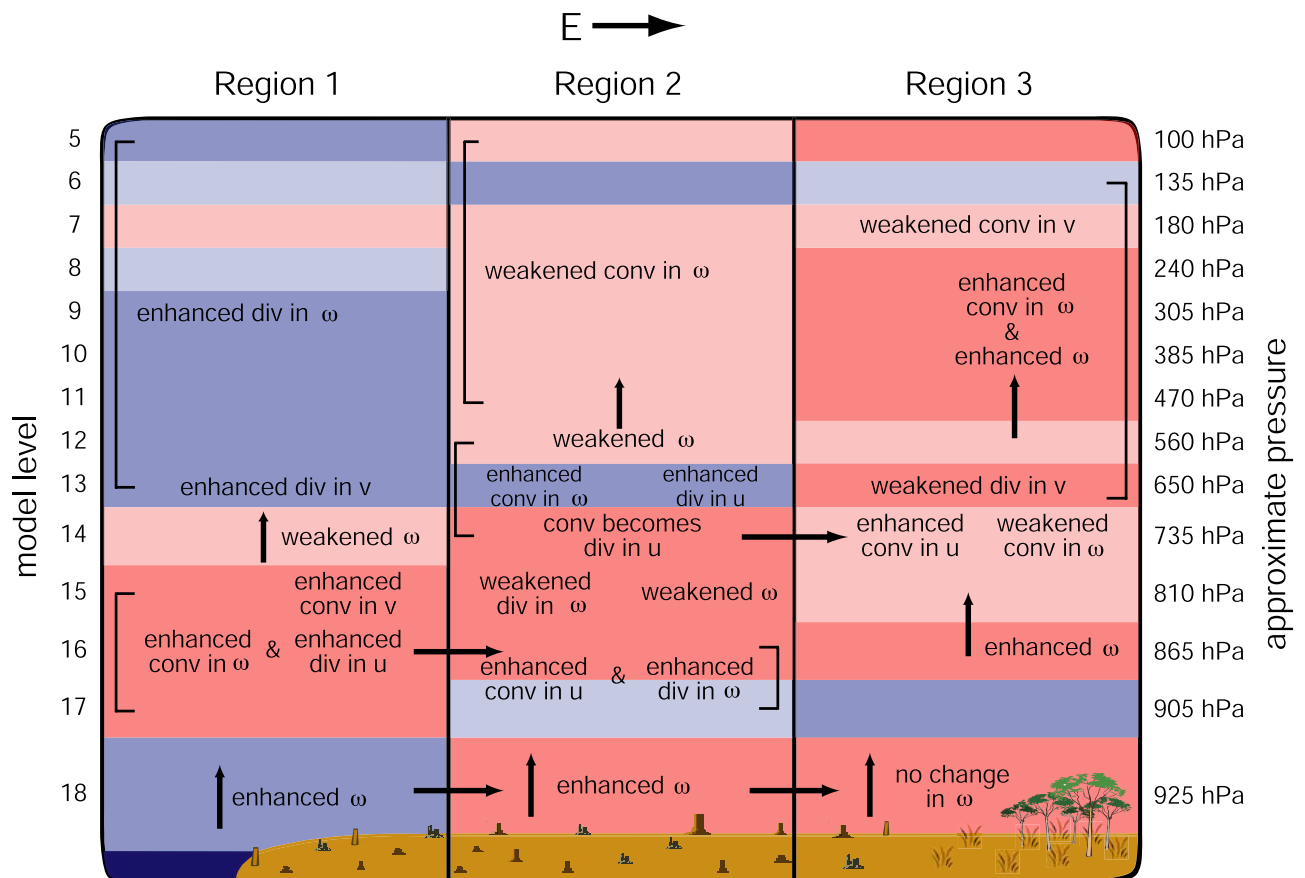


Figure 10. Qualitative summary illustrating the important changes in the energy budget between the three regions as a result of tropical forest removal. Dark blue regions depict areas of enhanced energy divergence (loss), while light blue regions depict areas of weakened energy divergence (gain). Dark pink regions depict areas of enhanced energy convergence (gain), while light pink regions depict areas of weakened energy convergence (loss). The letters “ u ,” “ v ,” and “ ω ” refer to zonal, meridional, and vertical directions of energy convergence or divergence, respectively. East is to the right.